university of groningen

University Medical Center Groningen

University of Groningen

The biology of human hematopoietic stem and progenitor cells in acute myeloid leukemia, aging and autologous transplantation

Woolthuis, Carolien Marthe

IMPORTANT NOTE: You are advised to consult the publisher's version (publisher's PDF) if you wish to cite from it. Please check the document version below.

Document Version
Publisher's PDF, also known as Version of record

Publication date:
2013

Link to publication in University of Groningen/UMCG research database

Citation for published version (APA):
Woolthuis, C. M. (2013). *The biology of human hematopoietic stem and progenitor cells in acute myeloid leukemia, aging and autologous transplantation*. s.n.

Copyright
Other than for strictly personal use, it is not permitted to download or to forward/distribute the text or part of it without the consent of the author(s) and/or copyright holder(s), unless the work is under an open content license (like Creative Commons).

The publication may also be distributed here under the terms of Article 25fa of the Dutch Copyright Act, indicated by the "Taverne" license. More information can be found on the University of Groningen website: https://www.rug.nl/library/open-access/self-archiving-pure/taverne-amendment.

Take-down policy
If you believe that this document breaches copyright please contact us providing details, and we will remove access to the work immediately and investigate your claim.

Downloaded from the University of Groningen/UMCG research database (Pure): http://www.rug.nl/research/portal. For technical reasons the number of authors shown on this cover page is limited to 10 maximum.

Download date: 19-04-2025

CHAPTER 8

Loss of stem cell quiescence and impaired stem cell function of $CD34^{+}/CD38^{low}$ cells one year following autologous stem cell transplantation

Carolien M. Woolthuis[1], Annet Z. Brouwers-Vos[1], Gerwin Huls[1], Joost Th. M. de Wolf[1], Jan Jacob Schuringa[1], Edo Vellenga[1]

[1] Department of Hematology, University Medical Center Groningen, University of Groningen, Groningen, The Netherlands

Submitted

Abstract

Patients following autologous stem cell transplantation (ASCT) are more susceptible to chemotherapy induced bone marrow toxicity. In the present study, bone marrow stem and progenitor cells were examined one year following ASCT and compared with normal bone marrow and mobilized peripheral blood stem cells (PBSC). Post-ASCT bone marrow contained a significant lower percentage of quiescent cells in the $CD34^+/CD38^{low}$ fraction compared to normal bone marrow. In addition, we observed a strongly decreased stem cell frequency in post-ASCT $CD34^+$ cells as defined by LTC-IC assays. Measurement of the levels of reactive oxygen species (ROS) by flow cytometry revealed comparable ROS levels in post-ASCT and normal bone marrow $CD34^+/CD38^{low}$ cells, while significantly higher ROS levels were observed in $CD34^+/CD38^{high}$ post-ASCT cells compared to normal bone marrow. Moreover, post-ASCT $CD34^+$ bone marrow cells demonstrated an increased sensitivity to BSO, a trigger for endogenous ROS production. Gene expression analysis on $CD34^+$ cells revealed a set of 195 genes, including HMOX1, EGR1, FOS and SIRPA that are persistently downregulated in PBSC and post-ASCT bone marrow compared to normal bone marrow. In conclusion, our data indicate that the diminished regenerative capacity of post-ASCT bone marrow is possibly related to a loss of stem cell quiescence and a reduced tolerability to oxidative stress.

Introduction

Autologous stem cell transplantation (ASCT) allows the application of high-dose chemotherapy and is included in the standard treatment regimens for multiple myeloma and relapsing lymphoma.[1;2] This strategy results in a considerably improved treatment outcome, but in 30-50% of the patients the underlying malignant disorder relapses.[3-5] In that case the treatment options are limited, in part due to a diminished capacity of the transplanted cells to recover from a next course of chemotherapy. Apparently, the applied chemotherapy and ASCT have resulted in an impaired chemotoxic stress response of the bone marrow cells.[6;7] These findings are in line with our recent observations demonstrating a shift within the $CD34^+$ progenitor cell compartment post-ASCT towards phenotypically defined granulocyte/macrophage progenitors (GMPs), which coincided with a reduced clonogenic potential and enhanced cell cycle activity.[8]

Mobilized peripheral blood stem cells (PBSC) have become the standard cell source for ASCT. During the growth factor induced stem cell mobilization, the hematopoietic stem cells (HSCs) egress from the bone marrow to the peripheral blood and are exposed to significantly higher oxygen levels compared to the bone marrow oxygen levels.[9-11] This change in oxygen levels might affect several cellular functions and can be a trigger to elevate the production of reactive oxygen species (ROS).[12] Experiments in mice have clearly demonstrated that higher ROS levels in the HSC fraction hamper stem cell function and promote differentiation to a more mature phenotype, associated with changes in cell cycle.[13] In turn, cell cycle changes were demonstrated to affect long-term engraftment.[14-16]

It is not well defined whether the infused PBSC can re-install their normal cellular programming following engraftment in the bone marrow, a process that might be required for proper stem cell function. Therefore stem cell quiescence and frequency together with ROS production of $CD34^+$ cells from post-ASCT bone marrow (one year following transplantation) were studied and compared to normal bone marrow cells and PBSC. In addition, gene expression profiling was performed to obtain more insight in underlying molecular mechanisms. The results indicate that the diminished regenerative capacity of bone marrow post-ASCT might be related to a loss of stem cell quiescence and enhanced ROS production by progenitor cells. In addition, micro-array studies demonstrated that changes in gene expression induced by mobilization are only partly restored in $CD34^+$ bone marrow cells post-ASCT.

Methods

Patient material

Bone marrow aspirates from patients one year following ASCT and normal controls were obtained after informed consent according to institutional guidelines. Potential donors for allogeneic bone

marrow transplantation and patients who underwent elective total hip replacement served as normal controls. PBSC material was obtained from patients who underwent apheresis for ASCT. The study was approved by the Medical Ethical Committee of the University Medical Center Groningen.

Flow cytometry analysis and sorting procedures

The mononuclear cell (MNC) fraction from bone marrow was isolated by density gradient centrifugation using lymphoprep (PAA, Cölbe, Germany). $CD34^+$ cells were isolated by EasySep immunomagnetic cell selection (StemCell Technologies, Vancouver, Canada) according to manufacturer's instructions. Sorting of $CD34^+$ bone marrow cells for long-term colony initiating cell (LTC-IC) experiments was performed by MoFLo sorting (Dako Cytomation, Carpinteria, CA, USA) using a CD34 PE-labeled antibody (Clone 8G12, BD Biosciences, San Jose, California, USA). The fluorescence activated cell sorting (FACS) analyses were performed on an LSR II flow cytometer (Becton Dickinson (BD), Alpen a/d Rijn, The Netherlands). Antibodies were obtained from BD. Data were analyzed using FlowJo (Tri Star, Inc, Ashland, OR, USA) software.

Hoechst and Pyronin Y staining

Cells were washed and resuspended in hematopoietic progenitor cell growth medium (HPGM) (Lonza, Leusden, The Netherlands). The staining was performed in this solution with 5 µg/ml Hoechst 33342 (Invitrogen) at 37˚C for 30 minutes, then 1.0 µg/ml Pyronin Y (Sigma) was added at 37˚C for an additional 45 minutes. Cells were washed in the solution containing Hoechst and Pyronin Y, followed by FcR blocking at 4˚C for 10 minutes. After staining with CD34-APC and CD38-Alexa700 at 4˚C for 20 minutes, cells were washed and analyzed.

Long-term culture initiating cell (LTC-IC) assay

For LTC-IC assays $CD34^+$ cells were plated in limiting dilution in a 96-wells plate precoated with MS5 stromal cells. Cells were expanded in LTC medium (α-minimum essential medium supplemented with heat-inactivated 12.5% fetal calf serum (Sigma, Zwijndrecht, The Netherlands), heat-inactivated 12.5% horse serum (Sigma), penicillin and streptomycin, 2 mM glutamine, 57.2 µM β-mercaptoethanol (Sigma) and 1 µM hydrocortisone (Sigma) supplemented with 20 ng/ml IL-3, 20 ng/ml granulocyte colony-stimulating factor (G-CSF) (Rhone-Poulenc Rorer, Amstelveen, The Netherlands) and 20 ng/ml thrombopoietin (TPO) (Kirin, Tokyo, Japan). Cultures were kept at 37 ºC and 5% CO2. Cultures were demi-depopulated weekly for medium change. After five weeks suspension cells were removed and methylcellulose (StemCell Technologies) supplemented with 20 ng/ml of interleukin-3, 20 ng/ml of interleukin-6 (both from Gist-Brocades), 20 ng/ml of G-CSF (Rhone-Poulenc Rorer), 20 ng/ml of c-kit ligand (Amgen), and 6 U/ml of erythropoietin was added. Two weeks later, wells containing CFCs were scored as positive and the LTC-IC frequency was calculated using L-Calc Limiting Dilution Software (StemCell Technologies).

Measurement of intracellular ROS levels

Intracellular ROS levels were determined by staining with the probe 5- (and 6)-chloromethyl-2',7'-dichlorodihydrofluorescein diacetate (CM-H2DCFDA; Invitrogen). Cells were suspended in a concentration of 10^6 cells/ml and CM-H2DCFDA was added to the cell suspension in a final concentration of 5 µM, followed by incubation at 37˚C for 30 minutes. Cells were washed and FcR blocking at 4˚C for 10 minutes was performed, followed by staining with CD34-PeCy7 and CD38-APC at 4˚C for 20 minutes. Thereafter cells were washed and analyzed. The mean fluorescence intensity (MFI) of CM-H2DCFDA was calculated using FlowJo and compared between groups.

In vitro treatment with buthionine sulfoximine (BSO)

$CD34^+$ normal bone marrow, post-ASCT bone marrow or PBSC cells were isolated and cultured in HPGM supplemented with 20 ng/ml IL3 and increasing concentrations of BSO. After three days of culture, cells were harvested, washed and counted for living cells. Thereafter colony forming cell (CFC) assays were performed in methylcellulose (StemCell Technologies) supplemented with 20 ng/ml of interleukin-3, 20 ng/ml of interleukin-6 (both from Gist-Brocades), 20 ng/ml of G-CSF (Rhone-Poulenc Rorer), 20 ng/ml of c-kit ligand (Amgen), and 6 U/ml of erythropoietin was added. Two weeks later, colonies were counted. To get insight in the sensitivity of human hematopoietic $CD34^+$ cells for BSO, the experiments were preceded by a titration experiment with $CD34^+$ cord blood cells incubated with increasing concentrations of BSO.

Gene expression profiling

Total RNA was isolated using the RNeasy micro kit from Qiagen (Venlo, The Netherlands) according to the manufacturer's recommendations. RNA quality was examined using the Agilent 2100 Bioanalyzer (Agilent Technologies, Waldbronn, Germany). Genome-wide expression analysis was performed on Illumina (Illumina, Inc., San Diego, CA) BeadChip Arrays Sentrix Human-12 v3 (46k probesets). Typically, 200ng mRNA for amplification with Illumina TotalPrep RNA Amplification Kit (Ambion) and 750ng of cRNA was used in labeling reactions and hybridization with the arrays according to the manufacturer's instructions. Data were analyzed using the BeadStudio v3 Gene Expression Module (Illumina, Inc.) and Genespring (Agilent, Amstelveen, The Netherlands). Clustering analyses were performed using Genespring GX10 software.

Statistical analysis

The Mann-Whitney U test was used for analysis of individual group differences. Differences with a P-value ≤ 0.05 were considered statistically significant.

Results

Patient characteristics

In order to get insight into the effects of the stem cell transplantation procedure on hematopoietic stem cell function, bone marrow cells from patients one year following ASCT (post-ASCT) were compared with normal bone marrow and PBSC. This study included post-ASCT patients with relapsing lymphoma (n=5) treated with intensive chemotherapy and ASCT using BEAM as conditioning regimen, multiple myeloma (MM) patients (n=16) treated with chemotherapy and ASCT using high dose melphalan as conditioning regimen. The median age of the included patients was 56 years (range 46-63 years). The infused autologous stem cell transplant consisted of at least 4.0 x 10^6 $CD34^+$ cells/kg (range 4.0-25.0 x 10^6). The peripheral blood cell counts at the time of study demonstrated a mean haemoglobin level of 8.2 mmol/l (range 6.5-10.0 mmol/l), a mean leukocyte count of 4.7 x 10^9/l (2.6-8.2 x 10^9/l), a mean granulocyte count of 2.6 x 10^9/l (1.3-5.0 x 10^9/l) and a mean platelet count of 145 x 10^9/l (59-239 x 10^9/l).

Reduced percentage of quiescent $CD34^+/CD38^{low}$ cells in bone marrow post-ASCT

An important characteristic of hematopoietic stem cells (HSCs) is their quiescent cell cycle status. To examine the effects of the ASCT procedure on stem cell quiescence one year post-ASCT, the percentage of cells in the G0 phase was measured by staining the cells with Hoechst and Pyronin Y followed by flow cytometric analysis. Both the $CD34^+/CD38^{high}$ and $CD34^+/CD38^{low}$ fraction were analyzed. Post-ASCT bone marrow cells (n=6) were compared with normal bone marrow cells (n=9) and mobilized peripheral blood stem cells (PBSC) (n=7). A representative sample of each group is shown in Figure 1A. Interestingly, post-ASCT bone marrow contained a significant lower percentage of quiescent cells in the $CD34^+/CD38^{low}$ fraction compared to normal bone marrow (mean percentage 23.6% (95%CI: 6.5-40.8%) vs. 48.6 (95%CI: 31.4-65.9%), p=0.045) (Figure 1B). Also $CD34^+/CD38^{low}$ PBSC cells demonstrated a lower percentage of quiescent cells (mean percentage 26.3% (95%CI: 8.4-44.2%)) compared to normal bone marrow, but this difference did not reach statistical significance (p=0.08). No significant differences in the percentage of quiescence cells were observed in the $CD34^+/CD38^{high}$ fraction between the three groups (Figure 1B).

In line with our previously published results,[8] $CD34^+/CD38^{low}$ cells of post-ASCT bone marrow demonstrated an increased percentage of cells in S/G2/M phase compared to $CD34^+/CD38^{low}$ cells of normal bone marrow (mean percentage 6.3 (95%CI: 0.25-12.4%) vs. 0.9% (95%CI: 0.17-1.64%), p=0.001).

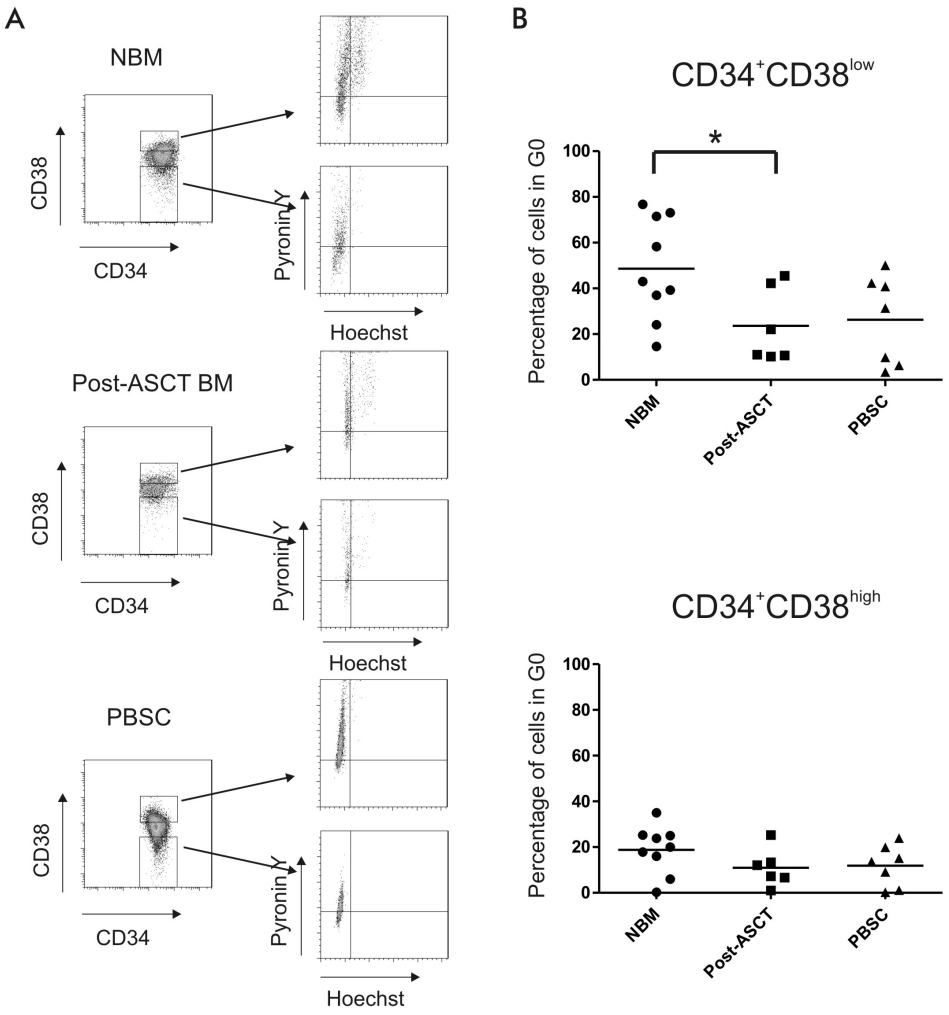

Figure 1 Reduced percentage of quiescent CD34⁺/CD38^{low} cells in bone marrow post-ASCT
*(A) Quiescence analysis of representative samples of normal bone marrow (NBM), post-ASCT bone marrow and PBSC. (B) Percentage of cells in G0 phase of cell cycle as analyzed for the CD34⁺CD38^{low} fraction (upper graph) and CD34⁺CD38^{high} fraction (lower graph). Horizontal lines indicate mean percentages per group. * p<0.05.*

Diminished stem cell frequency in CD34⁺ post-ASCT bone marrow cells

The reduced stem cell quiescence might imply a loss of stem cell function. Therefore the stem cell capacity of CD34⁺ cells from post-ASCT (n=5), PBSC cells (n=8) and normal bone marrow (n=11), was examined using *in vitro* long-term culture initiating cell (LTC-IC) assays. This analysis revealed a strongly decreased stem cell frequency in the CD34⁺ compartment of bone marrow post-ASCT compared to normal CD34⁺ bone marrow cells (mean frequency 0.0016 (95%CI: 0.0003-0.0028) vs.

0.0206 (95%CI: 0.0162-0.0250), p=0.002) (Figure 2). The stem cell frequency of CD34+ PBSC cells (0.0624 (95%CI 0.0173-0.1075)) was not significantly different from the frequency observed in normal bone marrow (p=0.12).

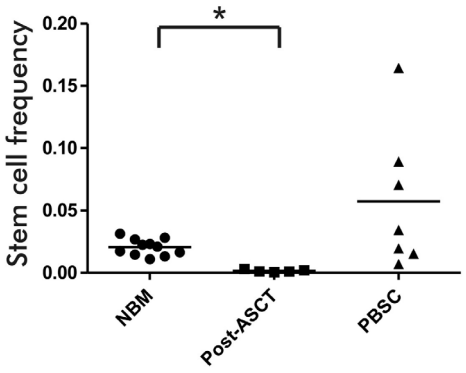

Figure 2 Strongly decreased stem cell frequency of CD34+ post-ASCT bone marrow
In vitro stem cell frequency was tested using the LTC-IC assay and results indicate the frequency in proportion as calculated by L-CALC in which for example a proportion of 0.025 indicates a stem cell frequency of 1 in 40. Horizontal lines indicate mean frequency per group. * p<0.01.

Increased ROS levels in CD34+/CD38high but not in CD34+/CD38low cells post-ASCT bone marrow cells

The mobilization procedure prior to ASCT implies the egression of hematopoietic stem and progenitor cells from the bone marrow to the peripheral blood. One of the factors that might contribute to the impaired stem cell function of post-ASCT bone marrow is an enhanced ROS production triggered by the changes in oxygen levels upon mobilization. To examine this in more detail, levels of reactive oxygen species (ROS) were measured by flow cytometric analysis in post-ASCT bone marrow (n=12), PBSC (n=7) and normal bone marrow (n=13). ROS levels in CD34+/CD38low post-ASCT bone marrow (mean MFI 8078 (95%CI 2823-13334)) were not significantly different from the levels observed in normal bone marrow cells. On the contrary, CD34+/CD38high post-ASCT bone marrow cells demonstrated higher ROS levels compared to normal bone marrow (mean MFI 12467 (95%CI 7606-17328) vs. 6430 (95%CI 4062-8799), p=0.014). In addition, significantly higher ROS levels were observed in CD34+/CD38low PBSC compared to normal bone marrow (mean MFI 10440 (95%CI 5153-15728) vs. 5194 (95%CI 2530-7857), p=0.043). ROS levels of both the CD34+/CD38low and CD34+/CD38high fractions of PBSC were not significantly different from those of post-ASCT bone marrow (Figure 3).

Increased sensitivity of CD34+ post-ASCT bone marrow cells to BSO treatment

To functionally test the effects of reactive oxygen stress on colony forming potential, CD34+ normal bone marrow, post-ASCT bone marrow and PBSC cells were treated with increasing concentrations of BSO followed by the CFC assay. Upon treatment with 20 μM BSO, CD34+ post-ASCT bone marrow cells demonstrated a significantly decreased ability to form CFU-GM colonies compared to

normal bone marrow (p=0.013), indicating increased sensitivity to oxidative stress. Although not statistically significant, comparable results were observed for 50 µM BSO treatment (Figure 4). When compared with CD34+ PBSC, a significantly decreased CFC potential of post-ASCT CD34+ cells was observed for all tested concentrations of BSO (Figure 4).

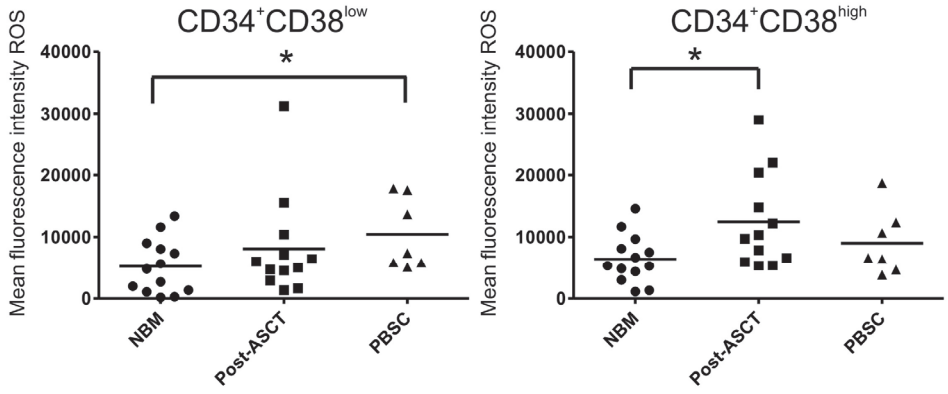

Figure 3 Increased ROS levels in CD34+CD38high post-ASCT bone marrow cells
Levels of intracellular reactive oxygen species (ROS) were measured by flow cytometric analysis and mean fluorescence intensity (MFI) of CM-H2DCFDA was calculated per sample. Analyses were performed for both the CD34+CD38low fraction (left graph) and CD34+CD38high fraction (right graph). Horizontal lines indicate the mean in MFI per group. * p<0.05.

Gene expression profiling

To define additional pathways affected by the ASCT procedure, micro-array analysis was performed comparing CD34+ cells from post-ASCT bone marrow (n=7), normal bone marrow (n=31) and PBSC (n=9). To identify gene expression changes that are induced by the mobilization procedure we first compared CD34+ cells derived from normal bone marrow versus CD34+ PBSC. This analysis revealed 1355 genes downregulated (fold change<0.75 and p<0.0001) and 1508 genes upregulated (fold change>1.5 and p<0.0001) in PBSC compared to normal bone marrow.

We were particularly interested in those gene expression changes that are associated with the mobilization procedure and remain affected in post-ASCT bone marrow. Especially those gene expression changes that appear to be irreversibly changed upon mobilization and transplantation are likely to contribute to the diminished stem cell frequency of post-ASCT CD34+ bone marrow. Analysis of the overlap of genes found to be downregulated in PBSC compared to normal bone marrow and in post-ASCT compared to normal bone marrow (551 genes (fold change<0.75 and p<0.0001)) revealed 195 genes to be downregulated in both PBSC and post-ASCT bone marrow compared to normal bone marrow (Figure 5A). The complete list of 195 genes is provided in Supplemental Table 1. A number of genes are of particular interest based on their known involvement in stem cell

maintenance, stem cell niche interactions and oxidative stress response, including HMOX1, EGR1, FOS and SIRPA (Figure 5B and 5D). GO analysis examining the list of 195 genes revealed that these genes may be involved in inflammatory and defense responses and cell adhesion among other things (Figure 5C). The decrease in HMOX1 expression in PBSC and post-ASCT bone marrow compared to normal bone marrow was confirmed by qRT-PCR (Figure 5E).

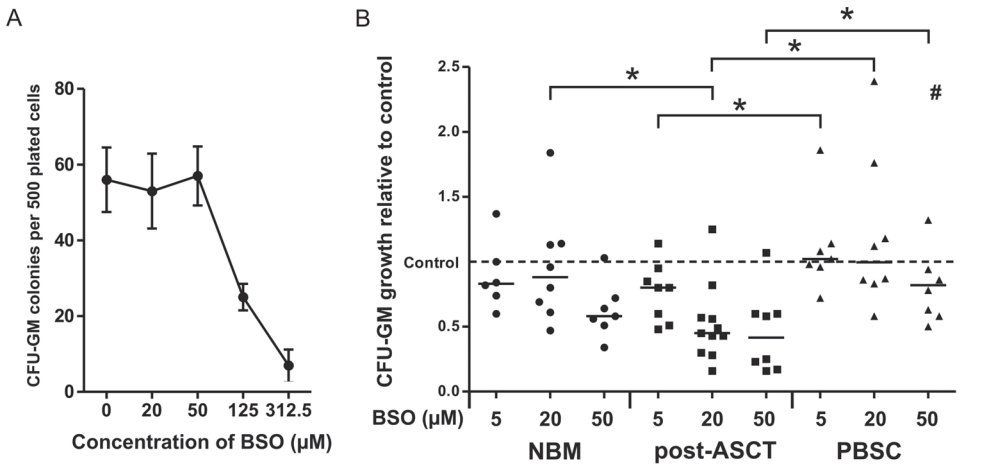

Figure 4 Increased sensitivity of CD34⁺ post-ASCT bone marrow to BSO

(A) Cord blood CD34⁺ cells were incubated with BSO in increasing concentrations followed by CFC-GM assay to determine the sensitivity of human hematopoietic CD34⁺ cells for BSO. Experiments were performed in duplo. (B) CD34⁺ normal bone marrow (NBM), post-ASCT bone marrow and PBSC cells were incubated with increasing concentrations of BSO and CFC-GM assays were performed. Results were corrected for the percentage of death cells after treatment and before plating cells for the CFC assays. Results are normalized for the results for no treatment per group, set to 1 (dashed horizontal line). * $p<0.05$, # outlier result for PBSC 50 µM (3.36) not shown in the graph. Horizontal lines indicate the median for each group.

Discussion

The results of our study reveal impairments in the hematopoietic stem cell compartment one year post-ASCT. These data might provide a basis for explaining the increased vulnerability to chemotherapy, an important clinical concern in patients post-ASCT. *In vitro* stem cell frequencies were reduced in CD34⁺ bone marrow cells one year post-ASCT. Moreover, the percentage of quiescent $CD34^{+}CD38^{low}$ cells was reduced. ROS levels were increased in the $CD34^{+}CD38^{high}$ cells post-ASCT, coinciding with an increased sensitivity to BSO of the total CD34⁺ cell fraction of post-ASCT bone marrow.

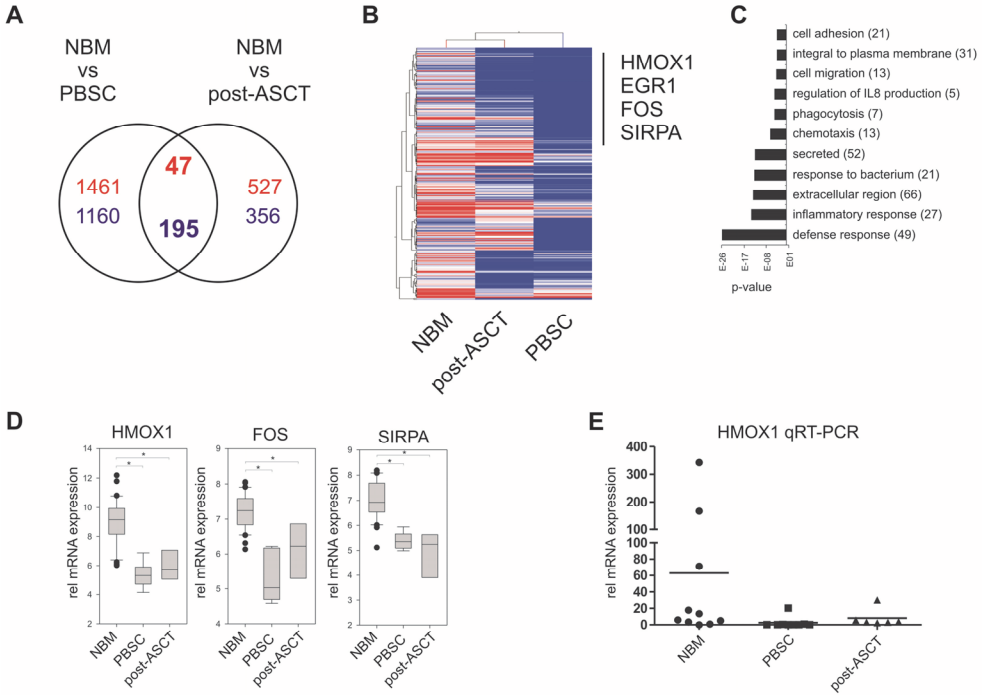

Figure 5 Gene expression changes in PBSC compared to normal bone marrow are not fully restored in post-ASCT bone marrow

(A) VENN diagram showing overlap in differentially expressed genes in PBSC versus normal bone marrow (left) and post-ASCT bone marrow versus normal bone marrow (right). Red indicates upregulated genes and blue downregulated genes. (B) Heat map indicating the gene expression changes wherein red color indicates relative high expression and blue color relative low expression. (C) GO analysis of 195 genes indicated in A. (D) Gene expression changes shown in detail for HMOX1, FOS and SIRPA. Statistically significant differences are indicated by an asterisk. (E) Results of an independent qRT-PCR analysis for HMOX1. Please note the two segments of the Y-axis with a different scale.

Our findings are in line with the concept that the hematopoietic compartment post-ASCT must be rebuilt and maintained by a limited number of HSCs. The nearly normal peripheral blood cell counts of patients post-ASCT indicate that the HSCs are able to maintain a stable supply of progenitors and differentiated hematopoietic cells. However, since stem cell frequencies were reduced post-ASCT it appears that these peripheral blood cell counts can only be generated via a higher cycling activity of the stem cell pool. We indeed observed that most HSCs post-ASCT have lost their quiescent cell cycle status. Although the underlying molecular mechanisms still need to be elucidated, it is possible that HSCs do not home properly to their quiescent niches in the bone marrow post-ASCT. Alternatively, it is also possible that cell intrinsic changes that are induced during the process of mobilization are not reverted back to their original state once HSCs are back in the bone marrow post-ASCT. Our gene array data on $CD34^+$ cells from normal BM, from mobilized PBSC and post-

ASCT bone marrow indeed indicate that a number of gene expression changes that were induced by the process of mobilization were not reversible. In particular, for a number of genes that were downregulated upon mobilization we observed that expression remained low in post-ASCT $CD34^+$ cells. Interestingly, this included genes such as HMOX1 and EGR1. EGR1 is an early response gene involved in cytokine regulation, in particular of IL8.[17] Mice that are haploinsuffcient for Egr1 demonstrate an increased susceptibility to chemotherapy-related leukemia.[18] Although loss of Egr1 does not impair reconstitution capacity in primary recipient mice, $Egr1^{-/-}$ HSCs exhibit premature loss of function during serial transplantation,[17;19] suggesting a protective function of EGR1 in the case of replicative stress. Also HMOX1 (HO-1) has been implicated in the stress response of HSCs. In line with the situation seen in patients post-ASCT, $HO\text{-}1^{+/-}$ mice demonstrate normal steady hematopoiesis but a blunted hematopoietic recovery following several courses of 5-FU treatment and a limited HSC reserve during long-term hematopoietic stress.[20] Other observed gene expression differences in post-ASCT bone marrow suggest a reduced interaction of $CD34^+$ cells post-ASCT with the bone marrow niche. The expression of genes from the group of integrins (ITGB2, ITGB5) as well as SIRPA are downregulated in PBSC and post-ASCT $CD34^+$ cells. The interaction of ITGB2 with ICAM1 was suggested to be important in the process of HSC engraftment in the bone marrow niche.[21] Also SIRPA was described as an important regulator of interactions between HSCs and the bone marrow niche.[22] The downregulation of these genes is probably necessary for the process of mobilization, but the downregulation in post-ASCT bone marrow might have negative effects on HSC function through an altered interaction with the micro-environment.

Oxidative stress has been reported to have diverse and sometimes detrimental effects on HSCs. Loss of stem cell quiescence has frequently been associated with increased levels of ROS production, which in turn triggers various cell biological effects ranging from DNA damage, p53-mediated apoptosis to enhanced cell cycle progression and differentiation of hematopoietic progenitors. Various key players have been identified that regulate oxidative stress in HSCs, including FoxO transcription factors,[12] BMI1[23] and HMOX.[20] While loss of FoxO resulted in increased cell cycling and apoptosis of HSCs,[12] $Gfi1b^{-/-}$ mice demonstrate elevated ROS levels but an expansion of the hematopoietic stem cell compartment.[24] So it seems that the context in which elevated ROS levels are present, will finally determine the consequences for the stem cell compartment. We also determined the ROS levels in stem and progenitor cells in normal BM, mobilized PBSC and in BM one year post-ASCT. While we observed a significant increase in ROS levels in the $CD34^+/CD38^{low}$ HSC compartment upon mobilization, no significant differences in ROS levels were observed in post-ASCT HSCs compared to normal BM HSCs. Interestingly, we did observe increased ROS levels in the $CD34^+/CD38^+$ progenitor compartment post-ASCT. Further future studies will be needed to determine the exact consequences of these increased ROS levels for progenitor cells post-ASCT.

Besides the strongly impaired capacity to recover from a second course of chemotherapy in case of relapsing disease, another major complication of ASCT is the occurrence of therapy-related myelodysplasia or acute myeloid leukemia (t-MDS/AML). Interestingly, Li et al. observed altered gene expression of genes related to mitochondria, oxidative phosphorylation and oxidative stress response in $CD34^+$ PBSC cells from patients who develop t-MDS/AML. Moreover, these cells were characterized by increased ROS generation, reduced ROS detoxification and enhanced DNA damage after therapeutic exposure.[25] Although examined from a different perspective, these data can be seen in line with ours and clearly support a theory in which the ASCT procedure induces an impairment of hematopoietic stem cell function characterized by oxidative stress defects.

In conclusion, our data indicate that the diminished regenerative capacity of bone marrow post-ASCT might be related to a loss of stem cell quiescence and enhanced ROS production by progenitor cells. Gene expression profiling revealed potential target genes of which the re-activation might improve the stress recovery capacity of post-ASCT bone marrow. Further studies aimed at identifying the molecular mechanisms contributing to the susceptibility of post-ASCT bone marrow may help in developing therapeutic interventions and improve this widely used treatment strategy.

References

1. Lokhorst HM, van der HB, Zweegman S et al. A randomized phase 3 study on the effect of thalidomide combined with adriamycin, dexamethasone, and high-dose melphalan, followed by thalidomide maintenance in patients with multiple myeloma. Blood 2010;115:1113-1120.

2. Vellenga E, van Putten WL, van ', V et al. Rituximab improves the treatment results of DHAP-VIM-DHAP and ASCT in relapsed/progressive aggressive CD20+ NHL: a prospective randomized HOVON trial. Blood 2008;111:537-543.

3. Lahuerta JJ, Mateos MV, Martinez-Lopez J et al. Influence of pre- and post-transplantation responses on outcome of patients with multiple myeloma: sequential improvement of response and achievement of complete response are associated with longer survival. J.Clin.Oncol. 2008;26:5775-5782.

4. Nademanee A. Transplantation for non-Hodgkin lymphoma. Expert.Rev.Hematol. 2009;2:425-442.

5. Palumbo A, Anderson K. Multiple myeloma. N.Engl.J.Med. 2011;364:1046-1060.

6. Nieboer P, de Vries EG, Mulder NH et al. Long-term haematological recovery following high-dose chemotherapy with autologous bone marrow transplantation or peripheral stem cell transplantation in patients with solid tumours. Bone Marrow Transplant. 2001;27:959-966.

7. Nieboer P, de Vries EG, Vellenga E et al. Factors influencing haematological recovery following high-dose chemotherapy and peripheral stem-cell transplantation for haematological malignancies; 1-year analysis. Eur.J.Cancer 2004;40:1199-1207.

8. Woolthuis C, Agool A, Olthof S et al. Auto-SCT induces a phenotypic shift from CMP to GMP progenitors, reduces clonogenic potential and enhances in vitro and in vivo cycling activity defined by (18)F-FLT PET scanning. Bone Marrow Transplant. 2011;46:110-115.

9. Parmar K, Mauch P, Vergilio JA, Sackstein R, Down JD. Distribution of hematopoietic stem cells in the bone marrow according to regional hypoxia. Proc.Natl.Acad.Sci.U.S.A 2007;104:5431-5436.

10. Suda T, Takubo K, Semenza GL. Metabolic regulation of hematopoietic stem cells in the hypoxic niche. Cell Stem Cell 2011;9:298-310.

11. Winkler IG, Barbier V, Wadley R et al. Positioning of bone marrow hematopoietic and stromal cells relative to blood flow in vivo: serially reconstituting hematopoietic stem cells reside in distinct nonperfused niches. Blood 2010;116:375-385.

12. Tothova Z, Kollipara R, Huntly BJ et al. FoxOs are critical mediators of hematopoietic stem cell resistance to physiologic oxidative stress. Cell 2007;128:325-339.

13. Jang YY, Sharkis SJ. A low level of reactive oxygen species selects for primitive hematopoietic stem cells that may reside in the low-oxygenic niche. Blood 2007;110:3056-3063.

14. Glimm H, Oh IH, Eaves CJ. Human hematopoietic stem cells stimulated to proliferate in vitro lose engraftment potential during their S/G(2)/M transit and do not reenter G(0). Blood 2000;96:4185-4193.

15. Gothot A, van der Loo JC, Clapp DW, Srour EF. Cell cycle-related changes in repopulating capacity of human mobilized peripheral blood CD34(+) cells in non-obese diabetic/severe combined immune-deficient mice. Blood 1998;92:2641-2649.

16. Szilvassy SJ, Meyerrose TE, Grimes B. Effects of cell cycle activation on the short-term engraftment properties of ex vivo expanded murine hematopoietic cells. Blood 2000;95:2829-2837.

17. Wilson A, Laurenti E, Trumpp A. Balancing dormant and self-renewing hematopoietic stem cells. Curr.Opin.Genet.Dev. 2009;19:461-468.

18. Joslin JM, Fernald AA, Tennant TR et al. Haploinsufficiency of EGR1, a candidate gene in the del(5q), leads to the development of myeloid disorders. Blood 2007;110:719-726.

19. Min IM, Pietramaggiori G, Kim FS et al. The transcription factor EGR1 controls both the proliferation and localization of hematopoietic stem cells. Cell Stem Cell 2008;2:380-391.

20. Cao YA, Wagers AJ, Karsunky H et al. Heme oxygenase-1 deficiency leads to disrupted response to acute stress in stem cells and progenitors. Blood 2008;112:4494-4502.

21. Peled A, Kollet O, Ponomaryov T et al. The chemokine SDF-1 activates the integrins LFA-1, VLA-4, and VLA-5 on immature human CD34(+) cells: role in transendothelial/stromal migration and engraftment of NOD/SCID mice. Blood 2000;95:3289-3296.

22. Takenaka K, Prasolava TK, Wang JC et al. Polymorphism in Sirpa modulates engraftment of human hematopoietic stem cells. Nat.Immunol. 2007;8:1313-1323.

23. Liu J, Cao L, Chen J et al. Bmi1 regulates mitochondrial function and the DNA damage response pathway. Nature 2009;459:387-392.

24. Khandanpour C, Sharif-Askari E, Vassen L et al. Evidence that growth factor independence 1b regulates dormancy and peripheral blood mobilization of hematopoietic stem cells. Blood 2010;116:5149-5161.

25. Li L, Li M, Sun C et al. Altered hematopoietic cell gene expression precedes development of therapy-related myelodysplasia/acute myeloid leukemia and identifies patients at risk. Cancer Cell 2011;20:591-605.

Supplemental table Woolthuis et al. 2013

symbol	av NBM total	av mobPBSC	av postASCT	fold mobPBSC/total NBM	t-test mobPBSC/total NBM	fold postASCT/NBM total	t-test postASCT/NBM total
ABCA13	8,32155129	5,999754286	5,689663333	0,16	2,42E-06	0,20	1,42E-04
ACP5	6,76467	5,336478571	5,654982222	0,46	8,19E-05	0,37	3,77E-05
ACPL2	6,553984194	5,848374286	6,026832222	0,69	3,18E-04	0,61	4,45E-04
ACTB	6,433759355	5,327465714	5,724086667	0,61	5,42E-04	0,46	3,19E-04
ADAM15	6,27578129	5,36007	5,659836667	0,65	9,78E-04	0,53	4,00E-04
ADAP1	6,225530323	4,536252857	4,600932222	0,32	9,21E-06	0,31	1,61E-04
ADAP2	7,435997742	5,701255714	4,625523333	0,14	8,08E-09	0,30	4,29E-04
ADSS	6,527470323	5,951797143	5,871286667	0,63	4,61E-04	0,44	2,29E-04
AGTRAP	6,934542258	5,624915714	4,594802222	0,20	6,79E-10	0,38	2,59E-04
AIF1	6,907847742	5,039271429	4,368733333	0,17	8,52E-10	0,55	2,03E-07
ALDH3B1	6,222241613	5,179077143	5,227152222	0,50	2,20E-04	0,49	7,22E-04
ANKRD22	7,705605484	6,043281429	5,647971111	0,24	1,77E-05	0,24	2,54E-04
ANKRD33	6,75255871	5,184742857	5,052297778	0,31	4,38E-08	0,34	6,85E-06
AOAH	6,741820645	5,485464286	5,254214444	0,36	3,74E-07	0,42	3,54E-04
APOBEC3A	7,499654839	5,650437143	5,530254444	0,26	2,33E-05	0,28	6,18E-04
APOE	9,586209677	7,207002857	5,011938889	0,04	1,84E-10	0,19	2,57E-04
ARAP3	7,228887419	5,186987143	4,728911111	0,18	1,20E-06	0,24	3,90E-04
ARG1	8,999475806	5,811642857	6,320593333	0,16	3,35E-04	0,11	1,66E-04
ARL6IP6	6,33015871	5,747415714	5,64162	0,62	8,26E-05	0,67	8,66E-04
ASCL2	6,714362258	5,641412857	5,859483333	0,55	2,69E-04	0,48	8,02E-04
ATP6V0E1	6,121984194	5,551238571	5,580114444	0,69	6,94E-05	0,54	9,97E-06
AZU1	9,983795484	6,845784286	3,079217778	0,01	5,48E-18	0,11	1,36E-05
B4GALT5	7,152230323	5,647335714	5,935271111	0,43	2,89E-04	0,35	4,30E-04
BCL6	7,33904129	5,871352857	5,669984444	0,31	9,98E-05	0,36	6,18E-04
BOK	6,395825484	5,514185714	5,669725556	0,60	1,18E-04	0,54	6,40E-05
BPI	10,43141065	6,130787143	5,632613333	0,04	2,13E-07	0,05	3,42E-05
C13orf15	6,843102581	4,800715714	4,602318889	0,21	9,00E-06	0,24	5,93E-04
C1orf162	7,054526774	5,199387143	5,501986667	0,34	1,05E-07	0,28	2,03E-06
C1QB	9,37478129	6,73427	4,900116667	0,04	6,56E-10	0,16	1,61E-04
C1QC	9,008492903	6,357537143	4,860121111	0,06	4,35E-09	0,16	1,55E-04
C5AR1	8,266470323	5,186018571	5,270234444	0,13	1,96E-06	0,12	1,85E-05
CA4	8,550195484	5,67056	6,569916667	0,25	8,71E-04	0,14	2,92E-05
CAMP	12,90178516	7,284908571	5,168162222	0,00	1,59E-13	0,02	3,16E-07
CD14	8,039202581	5,302457143	5,310414444	0,15	1,13E-05	0,14	4,16E-05
CD163	8,325372258	5,96316	4,230138889	0,06	3,76E-11	0,19	4,48E-05
CD300LF	6,615145484	5,213845714	5,755066667	0,55	3,54E-04	0,38	2,81E-05
CD33	6,164205161	5,130498571	4,523775556	0,32	1,52E-09	0,49	5,99E-04
CD68	7,184172258	4,793604286	4,824476667	0,19	3,91E-10	0,19	9,53E-08
CD93	6,873858387	5,296404286	4,927566667	0,26	6,09E-07	0,34	4,76E-04
CDA	8,41279871	5,209201429	5,857672222	0,17	2,62E-05	0,11	7,48E-06
CEACAM1	9,433828065	6,36261	6,835011111	0,17	6,38E-05	0,12	5,10E-05
CEACAM6	10,75947387	7,471102857	5,228363333	0,02	1,26E-09	0,10	3,26E-04
CEACAM8	11,57860645	6,890141429	5,921261111	0,02	8,92E-09	0,04	1,62E-05
CEBPD	7,384032903	4,945225714	4,280571111	0,12	8,48E-12	0,18	2,85E-06
CEBPE	8,351650645	6,260814286	5,613513333	0,15	2,63E-07	0,23	2,94E-04
CFD	6,396419677	4,620204286	3,334488889	0,12	4,85E-13	0,29	1,24E-04
CFP	6,850367097	4,574797143	5,258247778	0,33	3,48E-05	0,21	1,99E-06
CITED4	7,485838387	5,864884286	4,838752222	0,16	9,18E-09	0,33	6,35E-04
CKAP4	8,095048065	5,453762857	6,202692222	0,27	4,08E-04	0,16	5,10E-05

Supplemental table Woolthuis et al. 2013 (continued)

symbol	av NBM total	av mobPBSC	av postASCT	fold mobPBSC/total NBM	t-test mobPBSC/total NBM	fold postASCT/NBM total	t-test postASCT/NBM total
CLEC11A	7,396072903	6,256988571	5,952588889	0,37	1,77E-05	0,45	9,21E-04
CLEC12A	7,388551613	4,767001429	4,257395556	0,11	4,30E-11	0,16	1,75E-06
CLEC4A	7,088718387	5,776238571	4,882418889	0,22	1,86E-07	0,32	8,15E-04
CLEC7A	7,012329355	5,558738571	5,189013333	0,28	7,26E-06	0,37	7,15E-04
CNPY3	6,360948387	5,832562857	5,78011	0,67	5,17E-05	0,44	1,29E-04
CRISP3	8,451386129	6,284521429	6,131411111	0,20	1,62E-05	0,22	3,54E-04
CRISPLD2	7,706393226	5,196975714	5,262096667	0,18	2,82E-05	0,18	1,13E-04
CSF2RA	6,428432258	5,05829	4,803051111	0,32	8,17E-07	0,31	6,21E-05
CSF2RB	6,581914839	5,904125714	5,994752222	0,67	2,43E-04	0,63	1,69E-04
CSF3R	7,538340968	5,390611429	6,373773333	0,45	4,62E-05	0,26	2,38E-06
CST3	6,58557129	4,804612857	5,4445	0,45	1,56E-04	0,29	1,05E-05
CST7	8,086287097	5,884287143	5,303156667	0,15	1,52E-08	0,22	3,33E-04
CTSC	6,185276129	5,374482857	5,535371111	0,64	1,29E-05	0,54	8,90E-06
CTSG	9,539474516	7,51146	2,841586667	0,01	3,24E-20	0,25	1,29E-04
CTSH	7,372160323	4,957478571	3,537851111	0,07	1,07E-11	0,19	6,46E-05
CTSS	6,957854516	5,25395	5,39636	0,34	1,35E-04	0,31	3,54E-04
CTSZ	6,435780323	3,886177143	5,240101111	0,44	6,69E-07	0,17	1,73E-11
CXCL12	9,184455161	6,341402857	5,608622222	0,08	1,41E-08	0,14	1,89E-05
CXCL16	7,681224516	5,283495714	4,843554444	0,14	6,51E-08	0,19	2,77E-05
CYBA	6,77667	5,739181429	5,482881111	0,41	3,04E-08	0,49	8,39E-05
CYBB	8,093080968	5,260067143	4,334415556	0,07	1,36E-10	0,14	4,25E-06
CYP1B1	6,642945806	5,00504	5,019193333	0,32	9,76E-05	0,32	4,52E-04
CYP27A1	6,919475806	5,348717143	5,355222222	0,34	8,77E-05	0,34	5,25E-04
CYP4F3	9,514725484	6,116344286	5,922851111	0,08	4,04E-06	0,09	8,37E-05
DEFA1	13,35606323	9,521881429	7,562327778	0,02	1,13E-10	0,07	1,21E-05
DEFA1B	13,24448065	8,5971	6,925622222	0,01	1,07E-10	0,04	4,32E-06
DEFA3	13,41171839	9,259731429	7,168496667	0,01	7,09E-11	0,06	1,06E-05
DEFA4	12,5101671	7,550672857	5,627101111	0,01	9,04E-10	0,03	1,94E-05
DEGS1	6,452909677	5,59355	5,593623333	0,55	6,33E-05	0,55	3,73E-04
DYSF	8,157889677	5,080131429	5,229673333	0,13	8,57E-06	0,12	3,24E-05
EFHD2	6,48290871	5,644554286	5,452984444	0,49	3,37E-06	0,56	7,09E-04
EGR1	6,505464516	4,244062857	5,174267778	0,40	6,17E-04	0,21	2,18E-07
EHD4	6,282728065	4,988695714	5,245682222	0,49	1,22E-04	0,41	3,82E-05
ENTPD1	7,466179677	5,741952857	5,902563333	0,34	9,00E-05	0,30	2,06E-04
ERP29	6,393853226	5,229297143	5,683146667	0,61	8,92E-05	0,45	1,07E-04
FCER1G	7,393659677	4,624608571	5,771586667	0,32	2,18E-04	0,15	9,61E-06
FCGR2A	7,068353548	5,079382857	5,344476667	0,30	4,58E-04	0,25	3,36E-04
FCGRT	7,322214839	6,04799	5,330575556	0,25	5,80E-09	0,41	4,31E-04
FCN1	9,003022581	5,431441429	4,936313333	0,06	1,48E-08	0,08	1,87E-06
FEZ1	7,60754	5,854854286	5,216478889	0,19	3,48E-07	0,30	3,73E-04
FGL2	7,383285806	5,163545714	5,325901111	0,24	1,25E-05	0,21	7,98E-05
FGR	7,954832258	4,974152857	5,267331111	0,16	1,50E-06	0,13	1,93E-05
FOLR3	8,990517097	5,695772857	6,33366	0,16	1,81E-04	0,10	2,49E-05
FOS	7,190941935	6,217215714	5,291681111	0,27	7,54E-11	0,51	2,52E-04
FPR2	7,877283226	5,991318571	5,600273333	0,21	4,94E-06	0,24	2,07E-04
FTH1	6,466706452	4,905645714	5,20565	0,42	2,49E-05	0,34	2,68E-05
FTH1P3	6,453817097	5,160238571	5,422273333	0,49	2,80E-04	0,41	2,02E-04
FTL	6,511530968	5,462154286	5,717146667	0,58	2,48E-08	0,45	1,09E-09
FYB	6,794941935	4,651355714	4,605976667	0,22	3,33E-08	0,23	4,84E-06
G0S2	7,851855484	5,52589	5,700942222	0,23	2,50E-04	0,20	3,96E-04

Supplemental table Woolthuis et al. 2013 (continued)

symbol	av NBM total	av mobPBSC	av postASCT	fold mobPBSC/total NBM	t-test mobPBSC/total NBM	fold postASCT/NBM total	t-test postASCT/NBM total
GPX3	7,41200871	5,8247	5,937015556	0,36	1,12E-05	0,33	2,87E-05
GRN	7,007592258	5,079741429	5,135801111	0,27	8,77E-08	0,16	4,31E-07
HAL	7,017868387	5,830785714	4,788112222	0,21	1,63E-10	0,44	9,38E-04
HK3	8,88449129	5,280164286	5,535441111	0,10	4,90E-06	0,08	2,68E-05
HMOX1	8,97203129	5,976285714	5,347821111	0,08	3,96E-08	0,13	1,56E-05
HNMT	6,908043871	5,502328571	5,100937778	0,29	6,98E-07	0,38	2,61E-04
HOMER3	6,120052258	5,048561429	5,002326667	0,46	1,54E-05	0,48	2,77E-04
HTRA1	6,83078871	6,01253	5,83147	0,50	7,08E-06	0,57	3,18E-04
IFNGR2	6,59785	5,713884286	5,867697778	0,60	2,99E-04	0,54	1,48E-04
IL18RAP	8,280394839	5,706041429	5,750535556	0,17	3,85E-05	0,17	2,82E-04
IL6R	6,531151613	5,323748571	5,802413333	0,60	4,03E-04	0,43	9,84E-06
IMPA2	6,880695806	6,120998571	6,284571111	0,66	1,96E-04	0,59	3,29E-04
ITGAM	8,044194516	4,680144286	4,805886667	0,11	7,52E-07	0,10	1,66E-05
ITGB2	6,57021129	4,929485714	5,11121	0,36	1,06E-07	0,31	8,79E-06
ITGB5	6,900738065	5,230602857	5,345705556	0,34	5,84E-06	0,31	9,05E-06
KIAA0513	7,188236774	5,268594286	5,376376667	0,28	1,95E-05	0,26	5,73E-05
LCN2	12,12132581	6,694864286	7,862237778	0,05	2,02E-05	0,02	2,49E-06
LCP1	6,332807419	5,699855714	5,716927778	0,65	4,27E-05	0,64	2,78E-04
LGALS3	7,198373226	5,288358571	4,848172222	0,20	1,05E-06	0,27	5,47E-04
LGMN	8,801117097	7,061114286	5,362393333	0,09	2,83E-10	0,30	4,72E-04
LILRA3	8,324970968	5,455302857	6,36006	0,26	6,88E-04	0,14	2,54E-05
LTF	11,6325271	6,02391	5,860855556	0,02	7,29E-09	0,02	9,19E-07
LYZ	7,791408065	4,952348571	3,517504444	0,05	3,42E-12	0,14	1,58E-05
MAFB	7,359000645	5,360817143	5,053543333	0,20	3,22E-06	0,25	7,40E-05
MCOLN1	7,02911129	5,899094286	5,537102222	0,36	3,66E-07	0,46	3,04E-04
MMP8	9,935624516	6,292375714	6,901345556	0,12	1,42E-04	0,08	9,44E-05
MMP9	11,50409129	5,590815714	8,070632222	0,09	2,22E-04	0,02	9,16E-08
MNDA	8,731834839	5,109307143	4,869721111	0,07	1,41E-08	0,08	7,66E-07
MOSC1	8,044412903	6,201458571	5,55423	0,18	1,54E-09	0,28	3,66E-05
MS4A3	9,387369355	7,563885714	5,431442222	0,06	1,50E-10	0,18	2,10E-04
MS4A6A	7,565710645	4,99228	3,484454444	0,06	2,12E-13	0,17	1,23E-06
MS4A7	7,447897097	5,506465714	4,380077778	0,12	4,86E-09	0,26	2,26E-04
NCF1	8,184285161	5,504988571	4,761453333	0,09	2,51E-08	0,16	2,15E-05
NCF1C	7,938707742	5,966288571	5,021478889	0,13	1,50E-07	0,25	4,99E-04
NINJ2	6,740538065	5,615101429	5,09247	0,32	1,68E-07	0,46	7,41E-04
NKG7	7,34954129	5,072721429	5,263127778	0,24	6,95E-06	0,21	2,57E-04
NLRP12	7,40795129	5,50582	5,834478889	0,34	5,71E-04	0,27	3,35E-04
NPL	7,466334194	5,670435714	4,983744444	0,18	2,95E-07	0,21	2,64E-05
OLFM4	11,19265032	6,630488571	6,302944444	0,03	1,11E-06	0,04	8,64E-06
OLR1	9,56291871	5,818692857	5,557134444	0,06	5,98E-07	0,07	2,82E-05
OSCAR	7,403493548	4,972667143	4,982076667	0,19	2,77E-06	0,19	3,31E-05
P2RY13	7,370380645	5,889328571	5,999263333	0,39	2,43E-04	0,36	3,96E-04
PADI4	8,672577742	5,389884286	6,48596	0,22	1,24E-04	0,10	4,43E-06
PGLYRP1	11,54059677	6,673087143	7,470905556	0,06	1,63E-05	0,03	1,05E-05
PILRA	7,278649032	5,516362857	5,516421111	0,29	2,25E-05	0,29	2,62E-04
PLA2G16	6,806897419	5,327072857	5,089137778	0,30	1,58E-05	0,36	6,36E-04
PLA2G7	8,002092258	6,13003	5,156807778	0,14	7,88E-09	0,27	1,73E-04
PLAUR	6,928939677	4,920398571	4,972526667	0,26	1,41E-04	0,25	2,11E-04
PLBD1	9,379760645	5,19762	5,504044444	0,07	1,80E-07	0,06	9,98E-07
PPAP2B	7,601979677	6,140031429	6,192674444	0,38	1,16E-04	0,36	2,57E-04

Supplemental table Woolthuis et al. 2013 (continued)

symbol	av NBM total	av mobPBSC	av postASCT	fold mobPBSC/total NBM	t-test mobPBSC/total NBM	fold postASCT/NBM total	t-test postASCT/NBM total
PRAM1	7,025868065	5,109927143	5,98634	0,49	6,44E-05	0,26	7,38E-07
PRG3	10,85645645	6,614412857	5,236997778	0,02	1,67E-07	0,05	1,80E-04
PSAP	6,637111613	5,769098571	5,403456667	0,43	1,34E-07	0,55	9,33E-04
QPCT	8,545605484	5,70516	6,181717778	0,19	2,80E-04	0,14	2,13E-04
RAB31	7,839076774	5,372378571	4,95241	0,14	1,22E-08	0,18	2,90E-05
RAB32	6,77827871	5,261714286	5,760652222	0,49	1,19E-07	0,35	5,64E-07
RBP7	7,75614871	5,877074286	5,370886667	0,19	2,06E-07	0,27	6,95E-05
RETN	9,043876452	6,019657143	6,380925556	0,16	2,22E-04	0,12	2,26E-04
RGL4	8,128333871	6,162081429	6,370785556	0,30	3,56E-04	0,26	5,02E-04
RGS18	6,705690323	4,67994	5,329241111	0,39	5,49E-05	0,25	5,50E-07
RNASE2	8,697770645	6,70394	4,50162	0,05	2,67E-13	0,25	3,58E-05
RNASE3	10,52843903	7,255307143	4,437505556	0,01	1,94E-14	0,10	3,20E-06
S100A12	10,2937629	5,539534286	7,557914444	0,15	1,50E-04	0,04	1,37E-08
S100A9	9,016390968	5,431782857	6,988052222	0,25	3,05E-04	0,08	1,16E-10
S100P	9,740353548	5,458047143	6,67716	0,12	2,07E-04	0,05	5,34E-06
SASH1	6,617753548	5,817318571	5,424138889	0,44	1,95E-05	0,46	2,69E-04
SCPEP1	7,104859355	5,755248571	4,77664	0,20	4,01E-09	0,39	6,12E-04
SEC23B	6,51861871	6,062927143	5,810617778	0,61	2,47E-07	0,73	3,13E-04
SERPINA1	6,272117097	6,462355714	6,839343333	1,48	2,00E-04	0,13	5,35E-05
SERPINB8	6,958112258	6,120288571	5,410771111	0,34	9,34E-12	0,56	4,87E-04
SFT2D1	6,237126129	5,64092	5,754038889	0,72	1,03E-04	0,66	6,70E-05
SIGLEC5	7,471673871	5,605458571	5,948626667	0,35	5,23E-04	0,27	2,17E-04
SIRPA	7,004375484	4,90337	5,390172222	0,33	3,17E-07	0,23	2,21E-06
SLC15A3	7,619209355	5,392571429	4,635843333	0,13	1,32E-09	0,21	1,30E-05
SLC2A9	6,147995161	5,233362857	5,218198889	0,52	8,37E-07	0,53	1,17E-04
SLC39A11	6,376212903	5,448975714	5,538823333	0,56	6,20E-06	0,53	3,71E-04
SLC7A7	7,678756774	5,744728571	4,751767778	0,13	2,81E-07	0,26	7,70E-04
SLPI	8,994098065	6,326867143	6,098386667	0,13	4,00E-05	0,16	7,16E-04
SMPDL3A	7,521134839	5,719011429	6,139718889	0,38	1,10E-04	0,29	1,27E-05
SRGN	6,901626129	5,096811429	5,561677778	0,40	2,81E-08	0,29	4,82E-06
TBC1D9	6,850230323	5,68037	5,399407778	0,37	5,68E-07	0,44	6,26E-04
TCN1	10,36771387	6,325244286	6,2915	0,06	5,97E-06	0,06	5,78E-05
TFF3	9,878856774	6,363618571	5,70559	0,06	4,92E-08	0,09	2,22E-05
THBS1	6,175740968	4,046318571	4,497812222	0,31	9,26E-05	0,23	9,28E-06
TLR4	6,734787097	5,616668571	5,211498889	0,35	9,41E-08	0,46	1,31E-04
TLR8	7,092310323	5,118855714	4,874555556	0,21	3,78E-06	0,25	3,76E-04
TNFSF13	6,459030968	6,124035714	5,732035556	0,60	7,93E-04	0,50	2,83E-05
TNFSF13B	6,775489677	5,223807143	6,140054444	0,64	2,16E-04	0,34	4,32E-07
TRIB1	6,78976	5,12821	5,017084444	0,29	4,72E-04	0,32	6,42E-04
TUBB1	7,934534516	5,027222857	4,797065556	0,11	1,96E-07	0,13	5,91E-06
TYMP	7,000493548	4,733952857	5,640708889	0,39	9,69E-04	0,21	6,75E-05
TYROBP	7,199457419	4,016692857	5,204813333	0,25	8,22E-07	0,11	1,01E-07
VCAM1	10,62881935	7,917477143	5,157543333	0,02	2,85E-12	0,15	1,55E-04
VSTM1	8,091714194	5,930032857	5,227975556	0,14	1,33E-06	0,22	8,84E-04
WDR1	6,520894194	5,056038571	5,528291111	0,50	3,93E-04	0,36	5,89E-05
WLS	7,33860871	5,74504	5,585931111	0,30	1,40E-05	0,33	3,25E-04